https://dx.doi.org/10.1016/j.engstruct.2018.08.026

Mechanical behavior of high strength S690-QT steel welded sections with various heat input energy

Xiao Liu[1,2], Kwok-Fai Chung[1,2*], Ho-Cheung Ho[1,2], Meng Xiao[1,2] ,
Zhao-Xin Hou[3], and David A Nethercot[1,2,4]

[1] *Department of Civil and Environmental Engineering, and*
[2] *Chinese National Engineering Research Centre for Steel Construction (Hong Kong Branch),*
The Hong Kong Polytechnic University, Hong Kong SAR, China,
[3] *Chinese National Engineering Research Centre for Steel Construction, Beijing, China,*
[4] Department of Civil and Environmental Engineering, Imperial College London, U.K.
**Corresponding Author: Kwok-Fai.Chung@polyu.edu.hk*

ABSTRACT

Over the past two decades, there were a number of experimental investigations into mechanical properties as well as structural behaviour of high strength S690-QT steel welded sections. It is evident now that, similar to structural aluminium, these welded sections will suffer from a significant reduction in their mechanical properties, i.e. both yield and tensile strengths as well as ductility, due to change in microstructures if welding is not properly controlled. Owing to a lack of detailed understanding on effects of various welding procedures and parameters onto the mechanical properties of these steel welded sections, many design and construction engineers have serious concerns on adopting these S690-QT steel materials in buildings and bridges.

This project aims to investigate and quantify effects of various line heat input energy onto the mechanical properties of the S690-QT steel welded sections through a series of carefully planned and executed standard tensile tests. A total of 12 standard tensile tests on cylindrical coupons of welded sections were conducted, and full range deformation characteristics of these coupons were obtained through use of strain gauges and measurements on high resolution digital images. Both welding methods, namely, GMAW and SAW, were employed to prepare full penetration butt-welded sections with various line heat input energy. It should be noted that GMAW was performed with a robotic welding system while SAW was performed with an automated welding machine to attain high quality welding consistently. Additional standard tensile tests on 3 reference coupons machined from the base plates, and another 3 reference coupons machined from the weld metal were also conducted to provide basic material properties for direct comparison.

It was shown that in almost all coupons of the welded sections tested in the present study, fracture occurred within the heat affected zones of the welded sections without any failure in neither the weld metal nor the base plates. For welded sections prepared with a line heat input energy equal to 1.0 kJ/mm, there was almost no reduction in the mechanical properties of the welded sections. However, for those welded sections prepared with a line heat input energy equal to 5.0 kJ/mm, only 70% of the

yield strength of the base plates was attained. Consequently, the effects of welding onto the mechanical properties of the S690-QT steel welded sections have been successfully quantified, and the information is readily adopted in assessing their mechanical behaviour according to various line heat input energy employed during welding.

Keywords: High strength steel; welded sections; line heat input energy; strength reduction; and reduced ductility.

1. Introduction

With advances in metallurgical development and steel-making technology in many parts of the world over the past two decades, high strength steel materials with yield strengths above 460 N/mm^2 are commonly produced at affordable costs nowadays. High strength steel materials with yield strengths at 469, 690 and 960 N/mm^2 have been widely used in primary structural members of large lifting equipment and industrial machines because of their high strength-to-self-weight ratios. These steel materials are often considered to be highly attractive in construction by structural engineers because of their high structural economy (CEN, 2005). Willms (2009) summarized various manufacturing processes of different delivery conditions of these high strength steel materials. In general, there are three main delivery conditions for these steel materials: i) a normalized rolled process, ii) a quenched and tempered (QT) process, and iii) a thermo-mechanically controlled process (TMCP). Samuelsson and Schroter (2005) studied on historical developments of commonly available steel materials processed by different delivery conditions, and it is noted that high strength S690 steel materials are generally manufactured with the QT process. Nowadays, the high strength S690-QT steel materials are readily available for structural applications in many countries, and Tables 1 and 2 summarize chemical compositions and mechanical properties of these steel materials respectively (CEN, 2009a).

For many year, these high strength S690-QT steel materials are widely considered to be able to offer attractive structural solutions to those heavily loaded structural members in buildings or bridges. However, one of the major hindrances to their applications in construction is a concern of significant reductions in the mechanical properties of welded sections and joints, when compared with those of the base plates. As heating-cooling cycles during welding of these high strength S690-QT steel plates will cause adverse effects to the mechanical properties of the welded connections, especially in the vicinity of heat affected zones (HAZ), many design and construction have serious concerns on adopting these steel materials in buildings and bridges. In general, there is a lack of experimental evidence and design guideline for design and construction engineers to understand and to accept, and to be able to work with these high strength steel materials with a known level of confidence.

It should be noted that reductions in the mechanical properties of the high strength S690-QT welded sections are caused by changes in their microstructures in the vicinity of HAZ of the welded sections during welding. Similar behaviour in welded structural aluminium has been identified many years ago (Lai & Nethercot, 1992; Mazzolani, 1994), and since then, it is an important research topic for material characterization and processing engineering for many years. It should be noted that EN 1999-1-1 (2008) provides simple design rules to allow for reduction in resistances due to welding.

1.1. Welding of high strength steel plates

During welding of these high strength S690-QT steel plates, different types of microstructure grains are formed in both the weld metal and adjacent HAZ (Jenney and O'Brien, 2001). As summarized by

Krauss (1980) and Azhari et al. (2015; 2018), different metallurgical zones with different grain sizes were formed due to different maximum temperatures occurred during welding, and differential t_{8-5} values (i.e. cooling times in seconds from 800 down to 500 °C). Figure 1 shows a typical distribution of various metallurgical zones and corresponding phase-transition temperature variations during welding (Easterling, 1992). As microstructures of the S690-QT steel plates are very sensitive to the heat input energy employed during welding, significant reductions in both the yield and the tensile strengths of the HAZ of the welded sections will occur (Granjon, 1991; Jenney and O'Brien, 2001).

Mayr (2007) conducted a series of creep strength tests on high strength S690 steel welded sections with a design condition of "matching welding". Out of a total of 8 coupons tested, 7 of them were found to fracture at the HAZ, and hence, the HAZ was demonstrated to be the weakest zone in these welded sections due to changes in microstructures with the effects of welding.

A number of research studies (Jiao et al., 2004; Jiao et al., 2015; Amraei et al., 2016) were conducted to investigate the effects of HAZs on tension and compression resistances, hardness distributions, and plastic strain characteristics of butt-welded steel tubes made of different steel materials, including Grades 500, 960 and 1350. However, the line heat input energy was found to range from 0.43 to 0.81 kJ/mm. Lan et al. (2012) identified differences in microstructures and hardness of various HAZs while Ban and Shi (2017) summarized previous work on mechanical properties of welded connections made of S460 and S690 HSS. However, no information on the relationship between the strengths of these welded sections and the line heat input energy during welding was presented in both papers.

When considering the effects of heat input energy on HAZ of high strength steel welded section, Smith et al. (1989), Dong et al. (2014), and Ding et al. (2017) investigated various mechanical properties of the welded sections such as i) hardness, ii) toughness and iii) microstructures of HAZ under various line heat input energy. In general, all the mechanical properties of these welded sections were found to be reduced when the line heat input energy employed during welding increased though no specific relationships with yield and tensile strengths as well as ductility were established. More recently, Zhao et al. (2016) conducted a series of tensile tests on coupons of high strength S690-RQT steel welded sections, and a large reduction to the yield strength by up to 40% was obtained, when compared to that of the base plates. As the welding parameters were not provided, the corresponding line heat input energy employed during welding was not known. Nevertheless, it was shown that a strength reduction factor at 0.6 of the yield strength of these high strength steel materials was practically possible. These findings reinforced the need to quantify the effects of high input energy on various mechanical properties of high strength S690-QT steel welded sections.

1.2. Objectives and scope of work

In order to promote effective use of high strength S690-QT steel in construction, it is essential to investigate and quantify effects of welding onto their mechanical properties as well as structural

behaviour of welded sections and joints. This paper presents a detailed experimental study to determine the mechanical properties of a number of high strength S690-QT welded sections prepared with different line heat input energy employed during welding. The study takes the following forms of investigation:

a) To conduct standard tensile tests on cylindrical coupons of the welded sections prepared with various line heat input energy employed during welding.
b) To conduct standard tensile tests on similar reference coupons of both the base plates and the weld metal to provide basic mechanical properties for comparison.
c) To measure full range deformation characteristics of all these coupons.
d) To quantify reduction factors on various mechanical properties of the welded sections due to effects of welding.

A total of 18 standard tensile tests on cylindrical coupons were carried out, and both strain gauges and high resolution digital images of the coupons were used to provide full deformation characteristics of the coupons. The areas of interest of this study include:

- typical failure modes of HAZ of the welded sections under tension;
- reduction factors to both yield and tensile strengths, f_y and f_u , and to strains corresponding to tensile strength, ε_{fu} , and elongation at fracture ε_u ; and
- normalized true stress-strain relationships of the welded sections with different line heat input energy.

It should be noted that in order to attain high welding quality consistently in these welded sections, GMAW was performed using a robotic welding system with a low line heat input energy, as shown in Figure 2, while SAW was performed using an automated welding machine with a high line heat input energy, as shown in Figure 3.

2. Experimental investigation

2.1. Test programme

Standard tensile tests on cylindrical coupons were carried out to quantify reduction in the mechanical properties of the high strength S690-QT steel welded sections with the following line heat input energy, q :

i) 1.0 kJ/mm,
ii) 1.5 kJ/mm,
iii) 2.0 kJ/mm, and
iv) 5.0 kJ/mm.

It should be noted that for each line heat input energy, three coupons were tested. Hence, a total of 12 coupons of welded sections were tested. Additional standard tensile tests on 3 reference coupons of the base plates, and 3 reference coupons of the weld metal were also tested to provide basic mechanical properties for reference. All the test coupons were machined by a computer numerical control (CNC) machine to attain high accuracy in geometry. The machining procedures, including wire cutting, milling and grinding, were completed with sufficient volume of liquid coolants. Hence, all these procedures were controlled as cold machining processes. The test programme of a total of 18 standard tensile tests is presented in Table 3. Figure 4 illustrates the overall arrangement of the test coupons of i) the base plates, ii) the welded sections, and iii) the weld metal to be machined from a number of 16 mm thick welded sections. Detailed dimensions of various coupons are illustrated in Figure 5. All the dimensions of the coupons comply with various requirements given in BS EN ISO 6892-1 (CEN, 2009b).

2.2. Welding materials, procedures and parameters

In order to ensure that no failure will occur in the weld metal in all the coupons of the welded sections, a condition of "over-matched" welding is designed. According to recommendations of manufacturers, Electrode 'Lincoln 121K3C-H Plus' is used for GMAW while Electrode 'Lincoln LAC-690' is used for SAW. Nominal chemical compositions and mechanical properties of both electrodes are presented in Tables 1 and 2 respectively for direct comparison with those of the base plates.

It should be noted that all the base plates are 16.0 mm thick, and a V-notch is adopted for all welded connections. In order to control the magnitudes of the line heat input energy in these welded sections, different numbers of weld runs are prepared as shown in Figure 6, and the corresponding welding parameters of each of the weld runs for the welded sections with different line heat input energy are summarized in Table 4. Key parameters for welding include: i) a voltage, U and a current, I of an electricity provided to the welding arc; ii) a travel speed of the welding arc, v ; and iii) a heat input energy efficiency, □ .

It is shown that with proper control on the voltage and the current provided to the welding arc, the number of weld runs for line heat input energy per pass at 1.0, 1.5 and 2.0 kJ/mm are 4, 3 and 2 respectively when GMAW method is adopted. For a line heat input energy per pass at 5.0 kJ/mm, only 1 weld run is needed when SAW method is adopted. This ensures that for each welded section, the line heat input energy for each individual weld run is properly controlled throughout its entire length. All the welding parameters are carefully monitored and recorded during welding. It should be noted that the values of welding efficiency of GMAW and SAW methods are taken as 0.85 and 0.95 respectively (Singh, 2015). Hence, the measured average line heat input energy of these welded sections are found to be 0.97, 1.52, 2.03 and 4.94 kJ/mm respectively. All the coupons are then manufactured with precision machining to ensure that both the weld metal and the HAZ of the welded sections are located precisely at the centres of the coupons.

2.3. Test set-up, instrumentation and procedures

Figure 7 illustrates typical test set-up and instrumentation of a standard tensile test. Both the applied load and the corresponding elongation of the coupon are measured continuously throughout the test. The applied load is provided onto the coupon according to the following pre-determined loading rates at different deformation stages according to ISO 6892-1 (2009b):

a) Determination of Young's modulus: 100 N/mm^2/min
b) Determination of lower yield stress: 0.005 mm/mm/min
c) Determination of tensile strength: 0.03 mm/mm/min

It should be noted that two strain gauges were used to measure elongations of the coupon in the initial deformation stage of the test as they were able to measure elongations up to 5% precisely. High resolution digital photos on the entire gauge length of the coupon were captured at a regular time interval. With a fixed focal distance throughout a test, local deformations such as extension and necking of the coupon were readily obtained from counting pixels of the corresponding images once the elongations exceed 5%. Hence, both elongations and instantaneous diameters of the coupon were readily obtained.

3. EXPERIMENTAL RESULTS

All the tests have been successfully conducted, and they are terminated after fracture of the coupons. Deformed coupons of all the coupons are shown in Figure 8, and they are arranged in groups for easy comparison. After extensive data analysis, the experimental results of the tensile tests are presented as follows. It should be noted that all longitudinal strains were obtained by counting and comparing numbers of pixels in high resolution digital images captured during monotonic tests according to the digital image method proposed by Ho et al. (2018).

3.1. Tensile tests on reference coupons of base plates and weld metal

Figure 9 plots all the measured full range stress-strain curves of the reference coupons of both the base plates and the weld metal. Their measured mechanical properties are summarized in Table 5, and these include the Young's Modulus E, the yield strength f_y, the tensile strength f_u, the strain ε_{fu} at f_u, and the elongation at fracture ε_f. Averaged values of these mechanical properties are also provided for subsequent comparison. It is demonstrated that both the base plates and the weld metal are able to meet various ductility requirements stipulated in EN1993-1-12.

It should be noted that although the nominal yield strength of the base plates and the weld metal are 690 and 745 N/mm^2 respectively, their measured yield strengths are found to be 760.9 and 725.3 N/mm^2. Hence, a condition of "under-matched" welding is achieved despite a condition of "over-matched" welding is designed. Moreover, as shown in Figure 8, necking occurs at different locations

within the gauge lengths of all the 3 reference coupons of the base plates, and all the 3 reference coupons of the weld metal. Hence, no specific weak zone exists within the gauge lengths of these coupons.

3.2. Tensile tests on coupons of welded sections

Figure 10 shows all the fractured coupons after chemical etching, and boundaries of the HAZ are identified by visual inspection. It becomes evident that fracture occurs within the HAZ of the coupons and large elongations of the HAZ are apparent. Hence, there is a systematic weak zone existed within the HAZ of the welded sections despite the condition of "under-matched" welding is achieved in the welded sections.

Figure 11 plots all the measured stress-strain curves of the coupons of the welded sections prepared with different line heat input energy, and these curves are plotted onto different graphs according to their specific values of line heat input energy. In order to facilitate direct comparison, a representative curve is derived by averaging all the three measured stress-strain curves of the coupons of the welded sections under a specific line heat input energy. Similar to those of the base plates and the weld metal given in Table 5, all their measured mechanical properties are summarized in Table 6. Averaged values of these mechanical properties are also provided for subsequent comparison.

3.3. Comparison on deformation characteristics

All the representative stress-strain curves of the welded sections prepared with different line heat input energy employed during welding are plotted onto the same graph in Figure 12 together with those of reference coupons of the base plates and the weld metal for direct comparison. Similarly, all the reduced mechanical properties of the welded sections under different line heat input energy are summarized in Table 7 together with the mechanical properties of the base plates for easy comparison. Reduction factors for various mechanical properties of the welded sections are presented in Table 8.

It is shown that:

a) All the stress-strain curves of the base plates and the weld metal plotted in Figure 12 exhibit similar deformation characteristics though they deform to different limits. Hence, they behave in a linear elastic manner in the small deformation range, and then a highly non-linear manner with strain hardening in the large deformation range.

b) The four stress-strain curves of the welded sections prepared with different line heat input energy during welding are readily considered as non-linear modifications to the reference stress-strain curve of the base plates, as shown in Figure 12, that is, they have different levels of reduction in all the mechanical properties.

c) For the welded sections with a line heat input energy of 1.0 kJ/mm, the reduced yield strength is found to be 747.8 N/mm^2, which is very close to the yield strength of the base plate at 760.9 N/mm^2, as shown in Table 7. Similarly, the reduced tensile strength of the welded sections is found to be 808.3 N/mm^2, which is also very close to the tensile strength of the base plate at 809.5 N/mm^2. Hence, strength reduction to the base plates due to the effects of welding with a line heat input energy of 1.0 kJ/mm is very small.

d) As shown in Table 8, the reduced yield strengths for the welded sections with line heat input energy of 1.5, 2.0 and 5.0 kJ/mm are 0.90, 0.86 and 0.70 of that of the base plates respectively. Similarly, the reduced tensile strengths for the welded sections with line heat input energy of 1.5, 2.0 and 5.0 kJ/mm are 0.97, 0.92 and 0.83 of those of the base plates respectively. It is evident in these cases that strength reduction to the base plates due to the effects of welding is significant.

Both the reduced mechanical properties and the corresponding reduction factors presented in Tables 7 and 8 are plotted in Figure 14 to illustrate their variations with respect to the line heat input energy employed during welding. It is evident that these variations may be readily represented with a linear relationship.

4. CONCLUSIONS

In order to promote effective use of high strength S690-QT steel in construction, it is essential to investigate and quantify effects of welding onto their mechanical properties as well as structural behaviour of welded sections and joints. This project aims to investigate and quantify effects of various line heat input energy onto the mechanical properties of the S690-QT steel welded sections through a series of carefully planned and executed standard tensile tests. A total of 12 standard tensile tests on cylindrical coupons of welded sections were conducted, and full range deformation characteristics of these coupons were obtained through the use of strain gauges and measurements on high resolution digital images. Both welding methods, namely, GMAW and SAW, were employed to prepare full penetration welded sections with various line heat input energy. It should be noted that GMAW was performed with a robotic welding system while SAW was performed with an automated welding machine. Additional standard tensile tests on 3 reference coupons machined from the base plates, and another 3 reference coupons machined from the weld metal were also conducted to provide basic material properties for direct comparison.

It was shown that in almost all coupons of the welded sections tested in the present study, fracture occurred within the heat affected zones of the welded sections without any failure in neither the weld metal nor the base plates. Moreover, it is found that:

a) For welded sections prepared with a line heat input energy, q , equal to 1.0 kJ/mm, there is almost no reduction in the mechanical properties of the welded sections.

b) However, for those welded sections prepared with a line heat input energy, q, equal to 5.0 kJ/mm, only 70% of the yield strength of the base plates was attained.
c) In general, reduction factors to various mechanical properties are found to vary linearly according to the line heat input energy employed during welding.

Consequently, the effects of welding onto the high strength S690-QT mechanical properties of the S690-QT steel welded sections are successfully quantified, and the information us readily adopted in assessing their mechanical behaviour according to various line heat input energy employed during welding.

ACKNOWLEDGEMENT

The project leading to publication of this paper is partially funded by the Research Grants Council of the Government of Hong Kong SAR (Project No. PolyU 5148/13E, PolyU 152194/15E and PolyU 152687/16E) and the Research Committee of the Hong Kong Polytechnic University (Projects No. ZZCJ, RTK3 and RUQV). Both technical and financial support from the Chinese National Engineering Research Centre for Steel Construction (Hong Kong Branch) (Project No. 1-BBY3 & 6) of the Hong Kong Polytechnic University is also gratefully acknowledged. Special thanks go to the Nanjing Iron and Steel Company Ltd. in Nanjing for supply of high strength steel materials, and the Pristine Steel Fabrication Company Ltd. in Dongguan, Guang Dong for technical advice on automated welding. All the welded connections were fabricated at the Robotic Welding Laboratory of the Chinese National Engineering Research Centre for Steel Construction (Hong Kong Branch) with the robotic welding system *Fanuc i100* which was housed at the Industrial Centre of the Hong Kong Polytechnic University. Technical supports from the multi-skilled technicians of the Industrial Centre are gratefully acknowledged.

REFERENCES

ANSI. (2004). AWS D1.1:2004, Structural Welding Code - Steel. American National Standards Institute.

Amraei M, Skriko T, Björk T and Zhao XL. (2016), Plastic strain characteristics of butt-welded ultra-high strength steel (UHSS), Thin-Walled Structures, 109, 227-241.

Ban H, Shi G. (2017), A review of research on high-strength steel structures, Structures & Buildings, (2017), 1-17.

Dieter GE, & Bacon DJ. (1986). Mechanical metallurgy (Vol. 3). New York: McGraw-hill.

Dong H, Hao X, & Deng D. (2014). Effect of welding heat input on microstructure and mechanical properties of HSLA steel joint. Metallography, microstructure, and analysis, 3(2), 138-146.

Ding Q, Wang T, Shi Z, Wang Q, Wang Q, & Zhang F. (2017). Effect of welding heat input on the microstructure and toughness in simulated CGHAZ of 800 MPa Grade steel for hydropower penstocks. Metals, 7(4), 115.

Easterling KE. (1992). Introduction to the Physical Metallurgy of Welding 1992, Butterworth-Heinemann.

European Committee for Standardization. (2005). EN 1993-1-1: Design of steel structures, Part 1-1: General rules and rules for buildings.

European Committee for Standardization. (2007). EN 1993-1-12: Design of steel structures, Part 1-12: Design rules for high strength steel.

European Committee for Standardization. (2008). EN 1999-1-1: Design of aluminium structures: General structural rules.

European Committee for Standardization. (2009a). BS EN 10025-6, Hot rolled products of structural steels – Part 6: Technical delivery conditions for flat products of high yield strength structural steels in the quenched and tempered condition.

European Committee for Standardization. (2009b). BS EN ISO 6892-1, Metallic materials – Tensile testings, Part 1: Method of test at ambient temperature.

Granjon H. (1991). Fundamentals of Welding Metallurgy. Woodhead Pub. Ltd.

Ho HC, Liu X, Chung KF, Elghazouli AY, & Xiao M. (2018). Hysteretic behaviour of high strength S690 steel materials under low cycle high strain tests. Engineering Structures, 165, 222-236.

Jenney CL, & O'Brien A. (2001). Welding Handbook - Volumne 1: Welding Science and Technology. American Welding Society.

Jiao H and Zhao XL. (2004), Tension capacity of very high strength (VHS) circular steel tubes after welding. Advances in Structural Engineering – An International Journal, 7(4), 285-296.

Jiao H, Zhao XL and Lau A. (2015), Hardness and compressive capacity of longitudinally welded very high strength steel tubes, Journal of Constructional Steel Research, 114, 405-416.

Krauss G. (1980). Principles of heat treatment of steel. American Society for Metals.

Lai YFW, & Nethercot DA. (1992). Design of aluminium columns. Engineering structures, 14(3), 188-194.

Lan L, Qiu C, Zhao D, Gao X and Du L. (2012), Analysis of microstructural variation and mechanical behaviors in submerged arc welded joint of high strength low carbon bainitic steel, Materials Science and Engineering A, 558, 592-601.

Mayr P. (2007). Evolution of microstructure and mechanical properties of the heat affected zone in B-containing 9% chromium steels. PhD Thesis, Faculty of Mechanical Engineering,Graz University of Technology, Austria.

Mazzolani F. (1994). Aluminium alloy structures. CRC Press.

Smith NJ, McGrath JT, Gianetto JA, & Orr RF. (1989). Microstructure / mechanical property relationships of submerged arc welds in HSLA 80 steel. Welding Journal, 68(3), 11.

Samuelsson A. & Schröter F. (2005). High performance steels in Europe - Production processes, mechanical and chemical properties, fabrication properties. IABSE-Structural Engineering Document No. 8 - Use and application of high performance steels (HPS) for steel structures, 2005.

Singh R. (2015). Applied welding engineering: processes, codes, and standards. Butterworth-Heinemann.

Willms R. (2009). High strength steel for steel constructions. Nordic Steel Conferene.

Zhao MS, Chiew SP, & Lee CK. (2016). Post weld heat treatment for high strength steel welded sections. Journal of Constructional Steel Research, 122, 167-177.

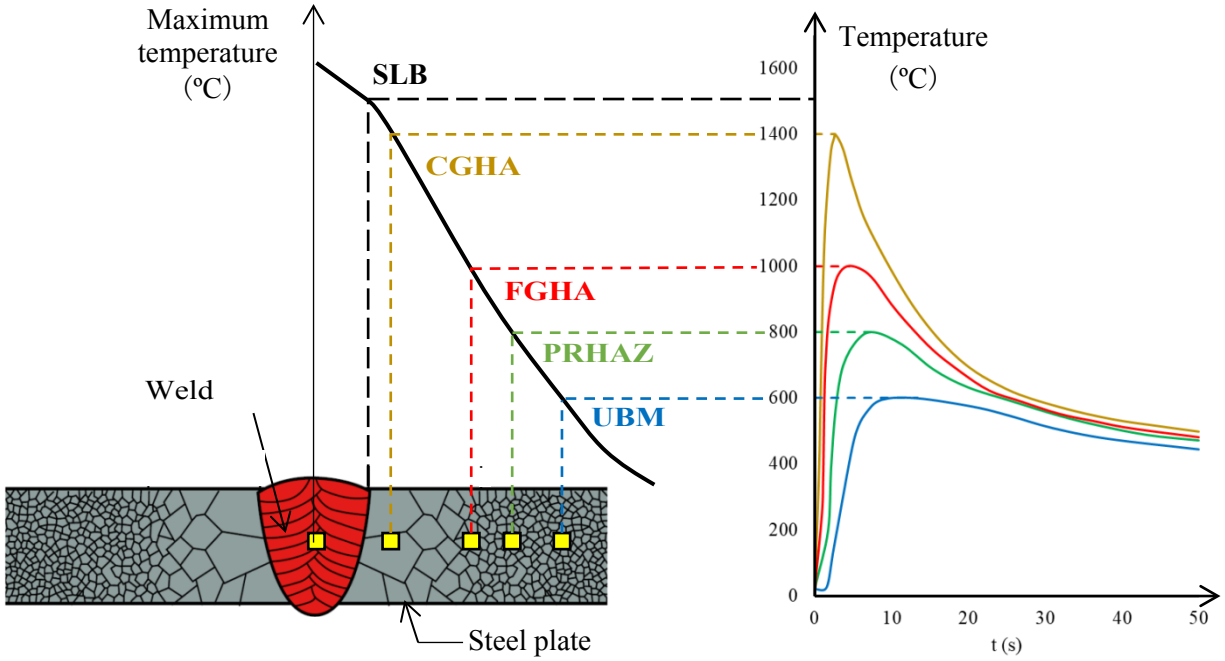

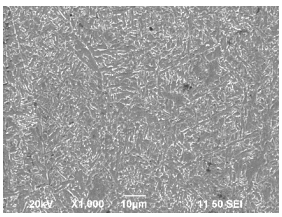

WM

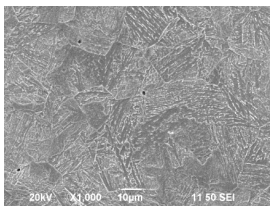

CGHAZ

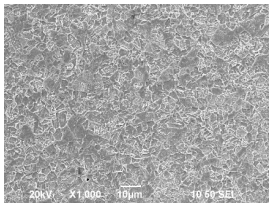

FGHAZ

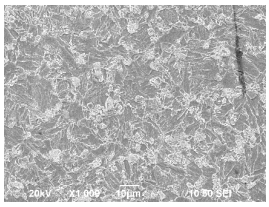

PRHAZ

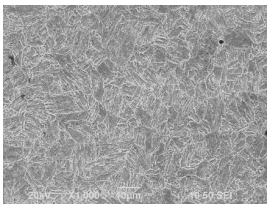

UBM

WM: weld metal
SLB: solid-liquid boundary
CGHAZ: coarse grain heat affected zone
FGHAZ: fine grain heat affected zone
PRHAZ: partially recyclized heat affected zone
UBM: unaffected base material

Figure 1. Metallurgical zones with different types of microstructures after welding

a) FANUC automatic welding robot

b) Temporarily fixing before welding

Figure 2. Robotic welding and typical set-up for GMAW welding

a) Automatic SAW welding

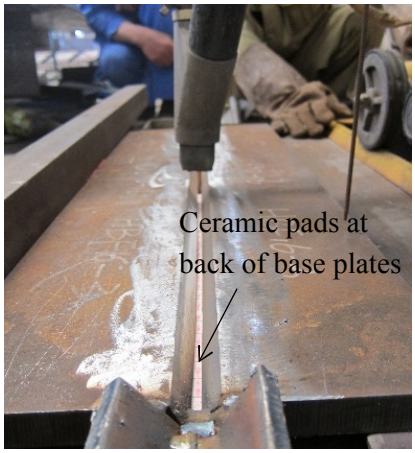

b) Typical set-up

Figure 3. Automatic welding and typical set-up for SAW welding

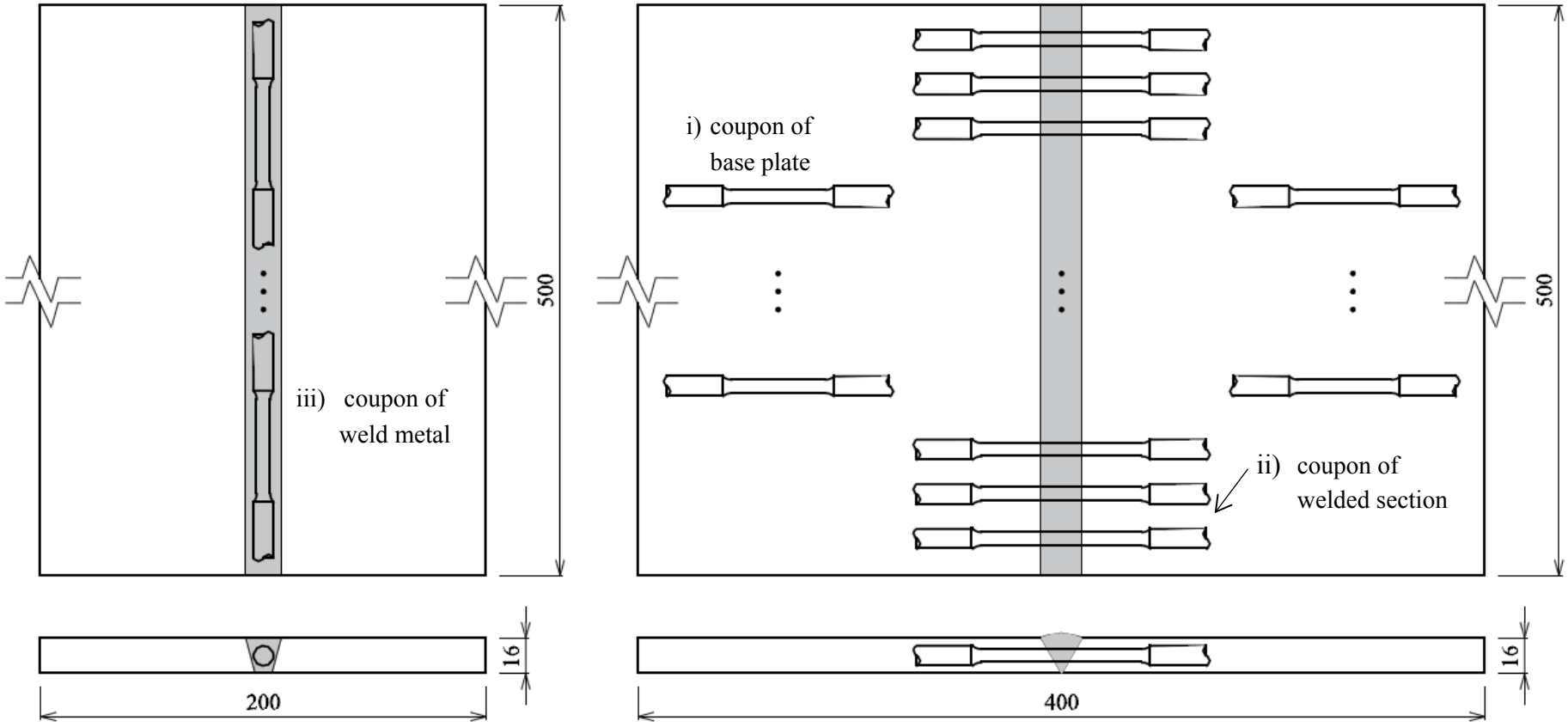

a) longitudinal coupons

b) transverse coupons

Figure 4. Arrangement of machined coupons from base plates, welded sections and weld metal

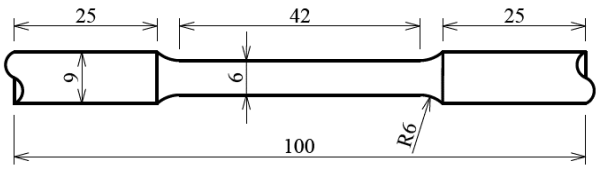

a) test coupon of base plate and weld metal

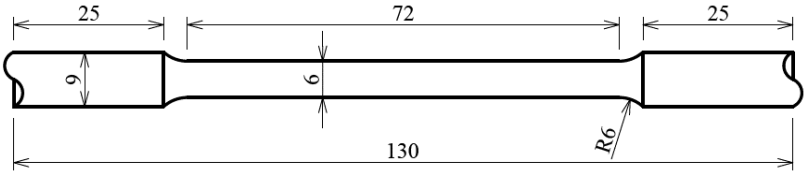

(b) test coupon of welded sections

Figure 5. Geometrical dimensions of coupons for various tests

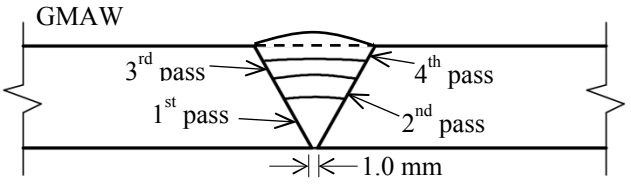

i) q = 1.0 kJ/mm

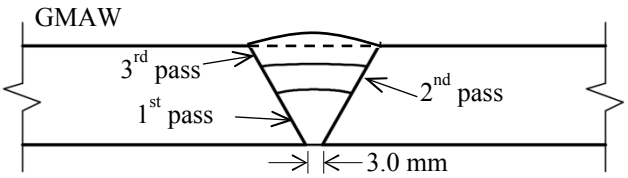

ii) q = 1.5 kJ/mm

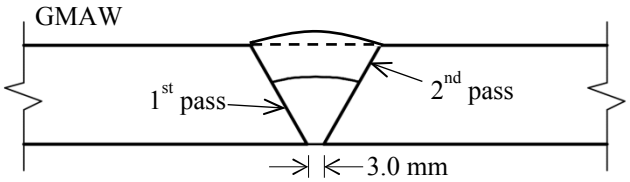

iii) q = 2.0 kJ/mm

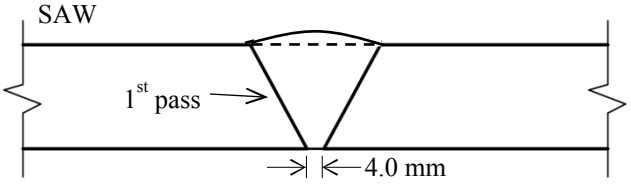

iv) q = 5.0 kJ/mm

Note: All 16mm thick plates.

Figure 6. Welding with different numbers of passes

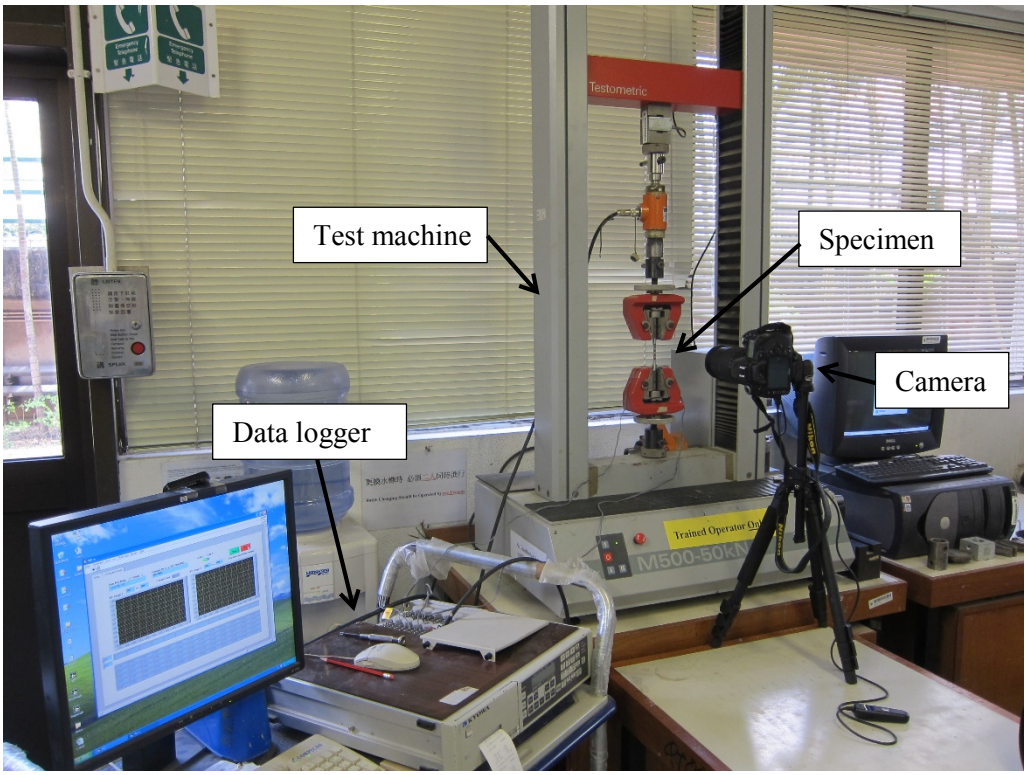

Figure 7. Test set-up of tensile tests

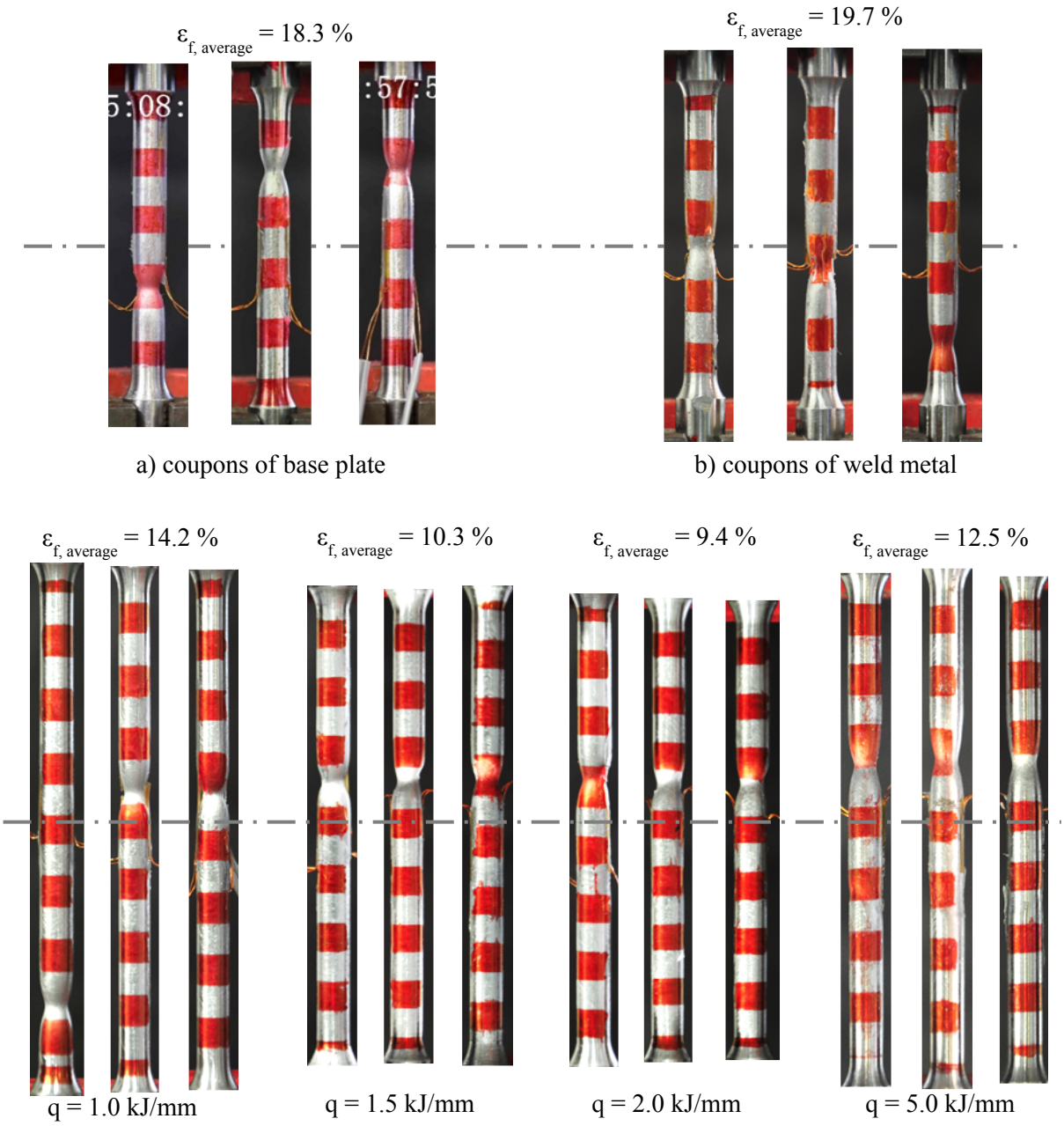

Figure 8. Local deformations and necking of all test coupons prior to failure

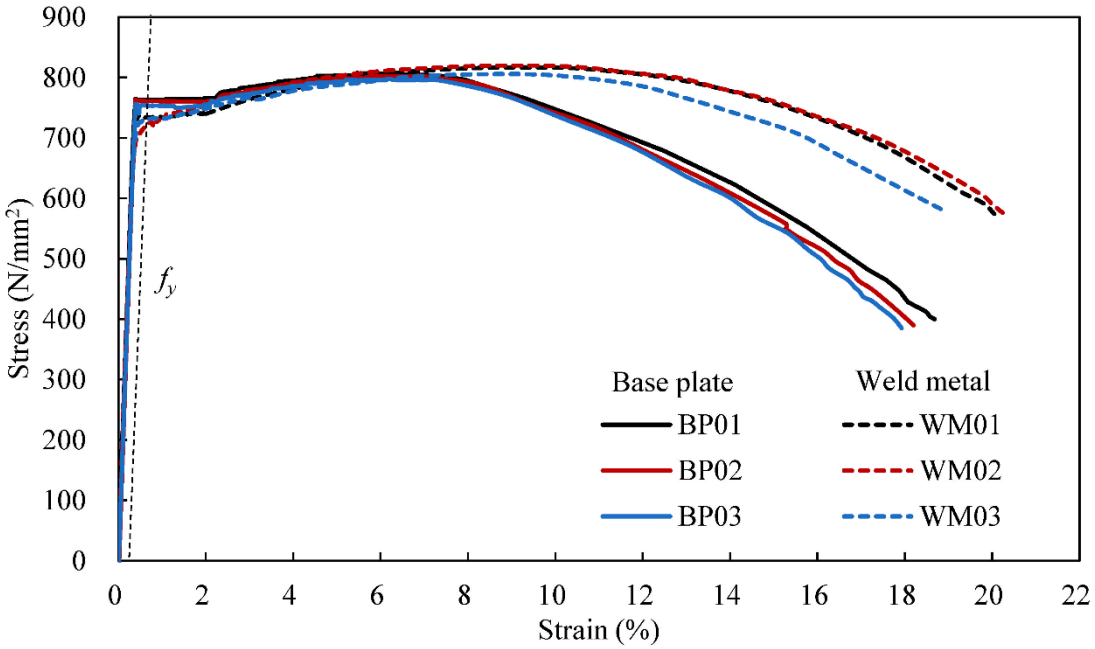

Figure 9. Full-range stress-strain curves of coupons of base plates and weld metal

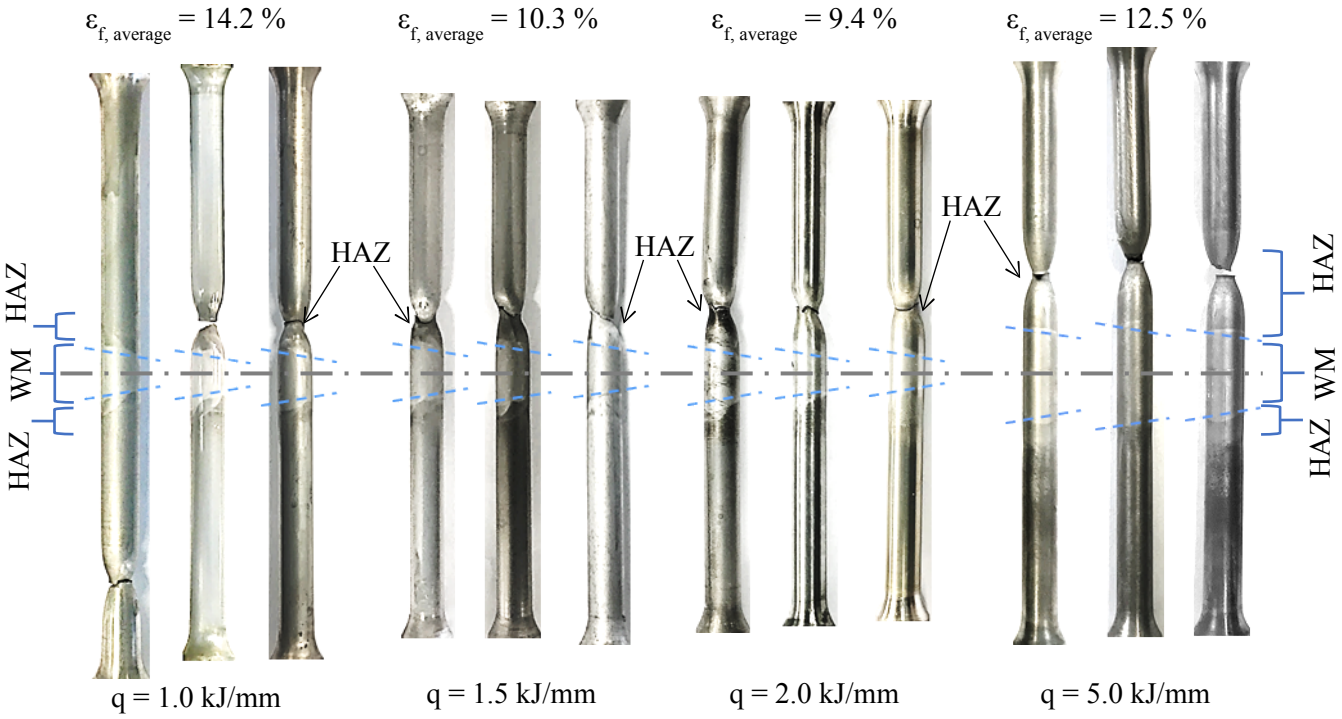

a) overall view

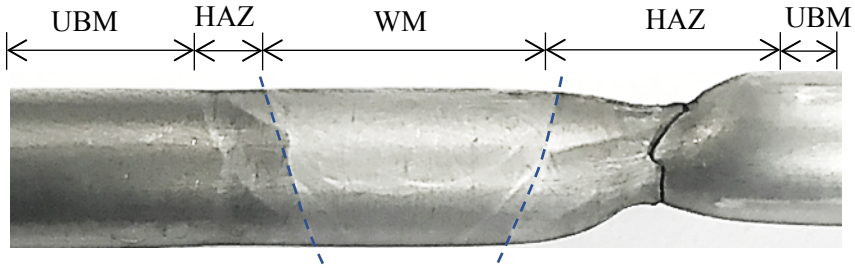

b) detailed view

Boundary of the weld metal

WM Weld metal

HAZ Heat affected zone

UBM Unaffected base material

Figure 10. Coupons after chemical etching and observed fracture location

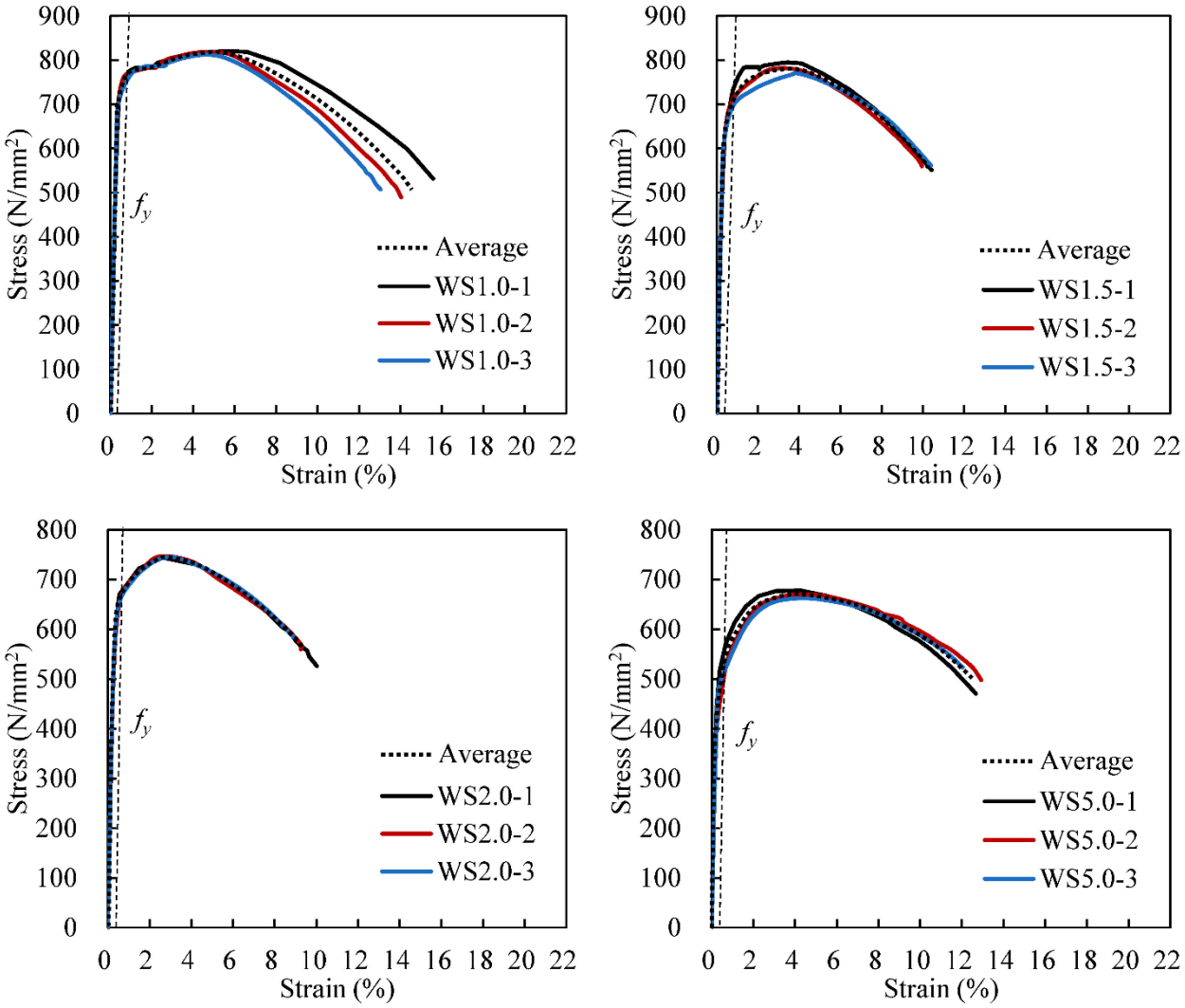

Figure 11. Full-range stress-strain curves of coupons of welded sections

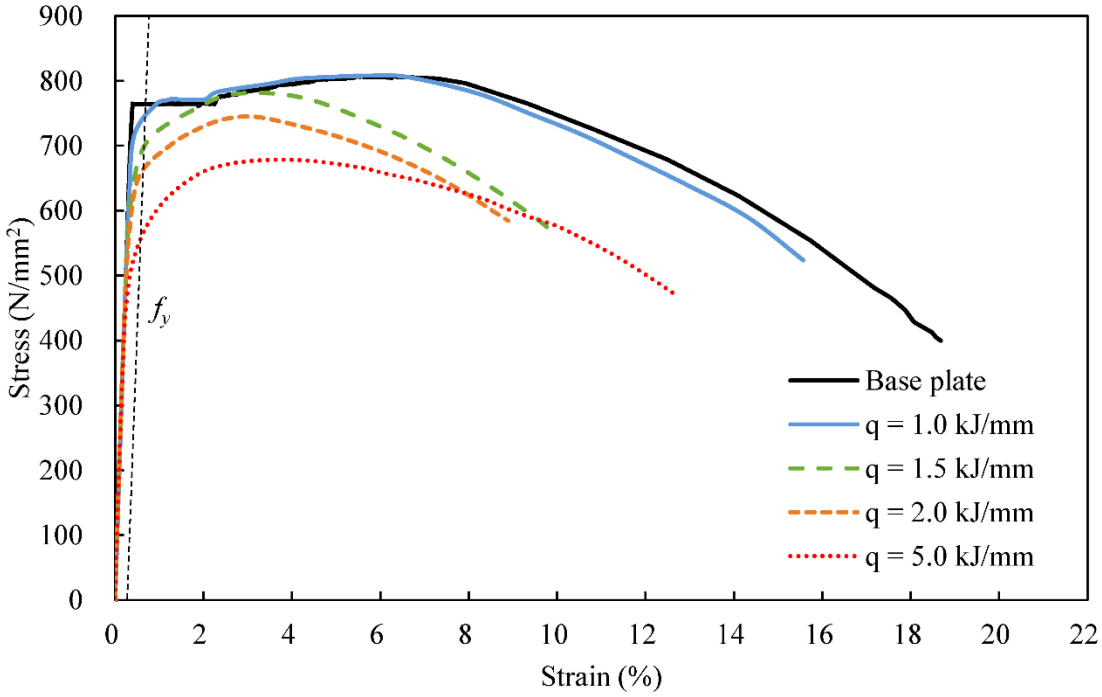

a) Full-range stress-strain curves

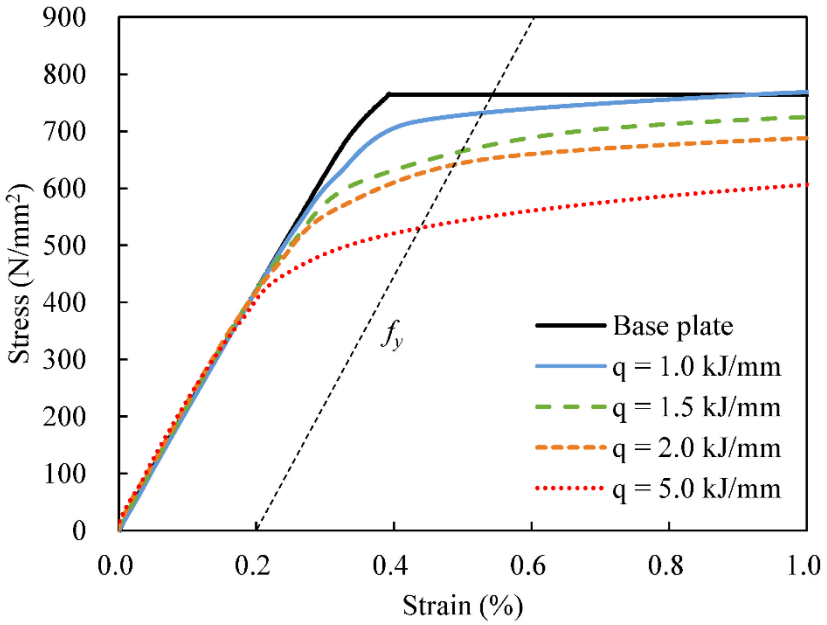

b) Linear range of stress-strain curves

Figure 12. Stress-strain curves of all coupons

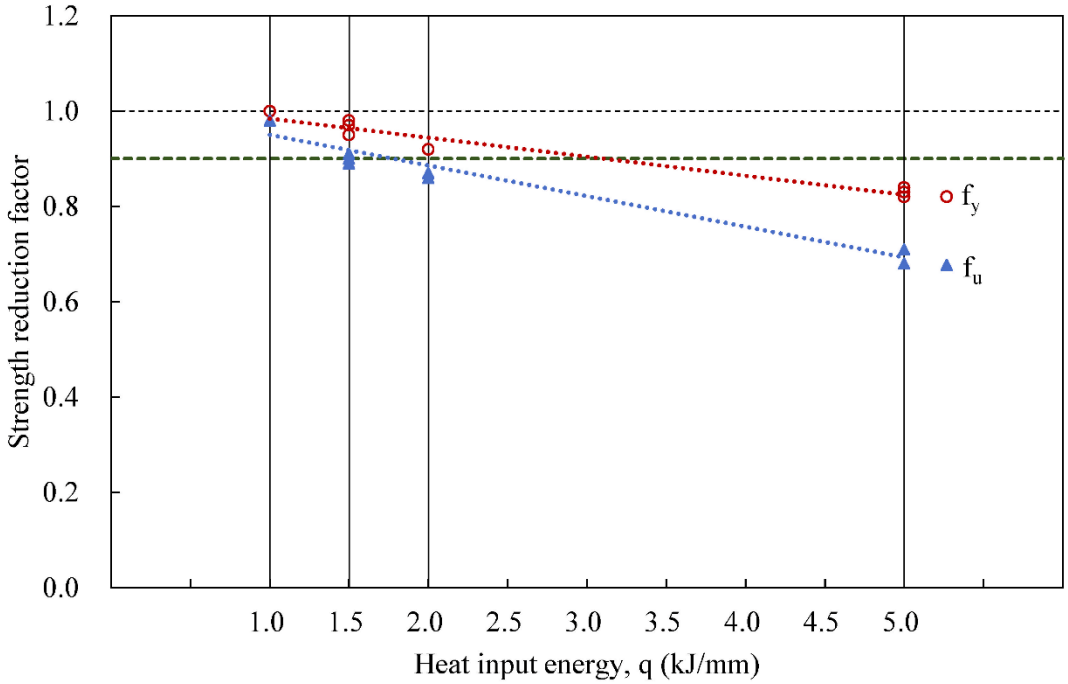

a) Strength reduction factors

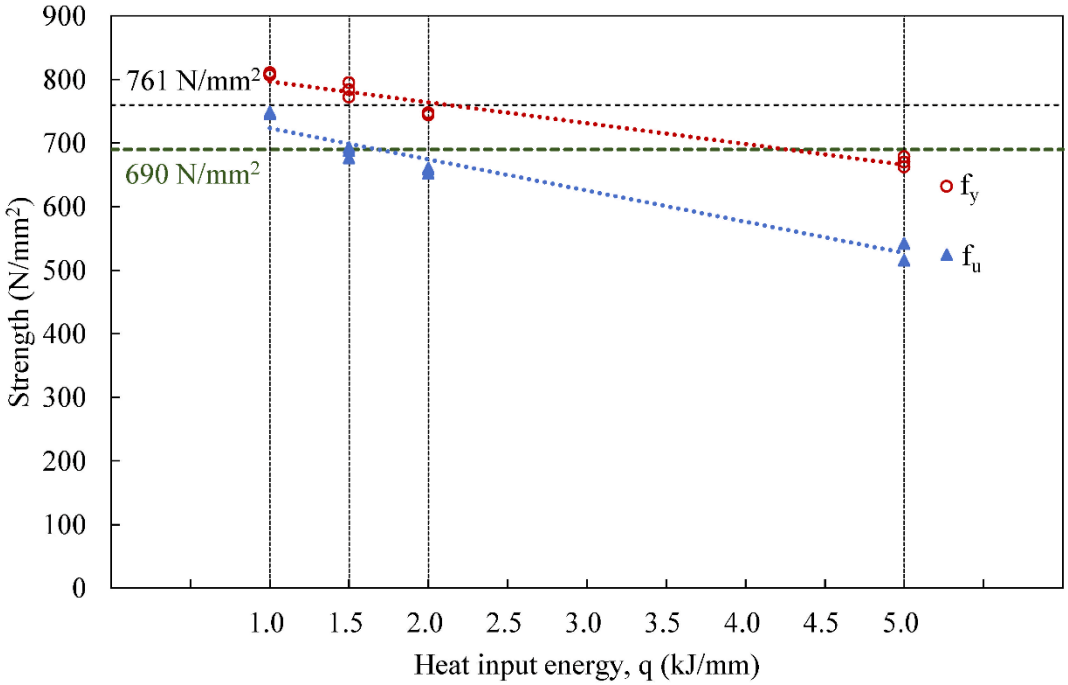

b) Reduced strengths

Figure 13. Reduced strengths and strength reduction factors for high strength S690-QT steel welded sections

Table 1. Nominal chemical compositions of base plates and welding materials

Material type	Electrode type	Chemical composition (%)								
		C	Mn	Si	S	P	Cr	Ni	Mo	Cu
Base plates	--	0.132	1.38	0.25	0.001	0.010	0.28	0.04	0.24	0.47
GMAW	Lincoln 121K3C-H Plus	0.070	1.88	0.29	0.012	0.011	0.07	2.50	0.65	-
SAW	Lincoln LAC-690	0.080	1.51	0.36	0.007	0.011	0.36	2.59	0.50	0.04

Table 2. Nominal mechanical properties of base plates and welding materials

Material type	Electrode type	Yield strength, f_y (N/mm^2)	Tensile strength, f_u (N/mm^2)	Elongation, $\square_f$ (%)
Base plates	--	≥690	≥770	≥10
GMAW electrode	Lincoln 121K3C-H Plus	≥745	≥825	≥14
SAW electrode	Lincoln LAC-690	≥758	≥830	≥20

Table 3. Test programme

Test	Steel grade	Diameter (mm)	Gauge length (mm)	Welding method	Welding materials	Heat input energy, q (kJ/mm)
BP	S690-QT	6	30	--	--	--
WS-1.0	S690-QT	6	30	GMAW	Lincoln 121K3C-H Plus	1.0
WS-1.5						1.5
WS-2.0						2.0
WS-5.0	S690-QT	6	30	SAW	Lincoln LAC-690	5.0

Notes: BP denotes coupons made from base plates, and
WS denotes coupons made from welded sections.

Table 4. Average values of welding parameters for welded sections

Welding type	Heat input energy, q (kJ/mm)	Voltage, U (V)	Current, I (A)	Welding speed, v (mm/s)	Efficiency, η	No. of passes	Computed heat input energy, q_c (kJ/mm)
GMAW	1.0	28.0	195	4.8	0.85	4	0.97
	1.5	25.9	228	3.3		3	1.52
	2.0	25.9	230	2.5		2	2.03
SAW	5.0	33.0	630	4.0	0.95	1	4.94

Notes: Heat input energy, $q = \eta \cdot U \cdot I / v$.

Table 5. Measured mechanical properties of the base plates and the weld metal

a) Test results on reference coupons of the base plates

Coupon type	Heat input energy, q (kJ/mm)	Specimen	Measured mechanical properties					
			Young's modulus, E (kN/mm^2)	Yield strength, f_y (N/mm^2)	Tensile strength, f_u (N/mm^2)	Strain at f_u, ε_{fu} (%)	f_u / f_y	Elongation at fracture, ε_f (%)
Base plate	-	BP01	208.8	752.2	808.4	6.7	1.07	18.5
		BP02	211.2	768.1	809.9	7.3	1.06	18.4
		BP03	210.1	762.4	810.3	6.5	1.06	17.9
		Average	210.0	760.9	809.5	6.8	1.06	18.3

b) Test results on reference coupons of the weld metal

Coupon type	Heat input energy, q (kJ/mm)	Specimen	Measured mechanical properties					
			Young's modulus, E (kN/mm^2)	Yield strength, f_y (N/mm^2)	Tensile strength, f_u (N/mm^2)	Strain at f_u, ε_{fu} (%)	f_u / f_y	Elongation at fracture, ε_f (%)
Base plate	-	BP01	203.6	733.7	818.0	8.8	1.11	20.0
		BP02	204.4	713.4	820.9	8.7	1.15	20.2
		BP03	203.0	728.9	806.1	8.3	1.11	18.8
		Average	203.7	725.3	815.0	8.6	1.12	19.7

Table 6. Test results on coupons of the welded sections under various heat input energy

Coupon type	Heat input energy, q (kJ/mm)	Specimen	Measured mechanical properties						Fracture position
			Young's modulus, E (kN/mm^2)	Yield strength, f_y (N/mm^2)	Tensile strength, f_u (N/mm^2)	Strain at f_u, ε_{fu} (%)	f_u / f_y	Elongation at fracture, ε_f (%)	
GMAW welded sections	1.0	WS1.0-1	208.9	749.1	807.9	5.7	1.08	15.6	Base plates
		WS1.0-2	209.9	748.4	810.8	4.8	1.08	14.0	HAZ
		WS1.0-3	207.8	745.9	806.3	4.8	1.08	13.0	HAZ
		Average	*208.9*	*747.8*	*808.3*	*5.1*	*1.08*	*14.2*	
	1.5	WS1.5-1	212.4	693.2	794.7	3.4	1.15	10.4	HAZ
		WS1.5-2	210.9	687.9	783.7	3.5	1.14	10.0	HAZ
		WS1.5-3	209.2	676.5	772.1	3.8	1.14	10.4	HAZ
		Average	*210.8*	*685.9*	*783.5*	*3.6*	*1.14*	*10.3*	
	2.0	WS2.0-1	204.8	658.7	744.0	2.7	1.13	10.0	HAZ
		WS2.0-2	211.3	660.6	747.7	2.6	1.13	9.3	HAZ
		WS2.0-3	206.1	652.4	744.8	3.1	1.14	8.9	HAZ
		Average	*207.4*	*657.2*	*745.5*	*2.8*	*1.13*	*9.4*	
SAW welded sections	5.0	WS5.0-1	184.3	541.6	678.6	4.3	1.25	12.7	HAZ
		WS5.0-2	203.6	542.4	669.8	4.1	1.23	12.9	HAZ
		WS5.0-3	221.8	515.7	662.1	4.3	1.28	12.0	HAZ
		Average	*203.2*	*533.2*	*670.2*	*4.2*	*1.25*	*12.5*	

Table 7. Reduced mechanical properties for welded sections under different heat input energy

Welding method	Heat input energy, q (kJ/mm)	Yield strength, f_y (N/mm^2)	Tensile strength, f_u (N/mm^2)	Strain at f_u, ε_{fu} (%)	Elongation at fracture, ε_f (%)
Base plate	---	760.9	809.5	6.8	18.3
GMAW	1.0	747.8	808.3	5.1	14.2
	1.5	685.9	783.5	3.6	10.3
	2.0	657.2	745.5	2.8	9.4
SAW	5.0	533.2	670.2	4.2	12.5

Table 8. Reduction factors for mechanical properties of welded sections

Welding method	Heat input energy, q (kJ/mm)	Reduction Factors, α			
		Yield strength, f_y (N/mm^2)	Tensile strength, f_u (N/mm^2)	Strain at f_u, ε_{fu} (%)	Elongation at fracture, ε_f (%)
GMAW	1.0	0.98	1.00	0.75	0.78
	1.5	0.90	0.97	0.53	0.56
	2.0	0.86	0.92	0.41	0.51
SAW	5.0	0.70	0.83	0.62	0.68

Notes: Yield strength ratios $= f_y / f_{y\_BP}$,
Tensile strength ratios $= f_u / f_{u\_BP}$,
Enlogation ratios $= \varepsilon_f / \varepsilon_{f\_BP}$.